JOURNAL OF GUIDANCE, CONTROL, AND DYNAMICS
Vol. 21, No. 3, May–June 1998

Time-Frequency Analysis for Transfer Function Estimation and Application to Flutter Clearance

E. Feron*
Massachusetts Institute of Technology, Cambridge, Massachusetts 02139
M. Brenner†
NASA Dryden Flight Research Center, Edwards, California 93523-0273
and
J. Paduano‡ and A. Turevskiy§
Massachusetts Institute of Technology, Cambridge, Massachusetts 02139

A transfer function estimation procedure that relies on the time-frequency analysis of input and output signals is described. This method was developed in an attempt to better identify the aeroelastic behavior of NASA Dryden's F-18 systems research aircraft and to predict its flutter boundaries using in-flight experimental data. Numerical experiments on field data show that exploiting the time-frequency characteristics of the excitation inputs can bring enhanced accuracy and confidence when identifying multi-input/multi-output transfer functions. In particular, the proposed approach complements many well-established black-box identification procedures by providing an independent way to obtain transfer function estimates. A computational tool implementing this approach is now being evaluated for practical use at NASA Dryden Flight Research Center.

Nomenclature

$b(w)$	= passband filter
h_i	= transfer function from input i to the output
$\tilde{h}_{l,i}$	= estimated transfer function from left input to the output for i data set
$\tilde{h}_{r,i}$	= estimated transfer function from right input to the output for i data set
J_{ij}	= cost function
$\mathcal{TF}$	= time-frequency representation of a signal
$\mathcal{TFW}$	= denoised time-frequency representation of a signal
U_i	= discrete Fourier transform (DFT) of a denoised time-frequency representation of an input signal
u_i	= input signals
$\hat{u}(j\omega)$	= DFT of a signal
$u(t)$	= signal in time domain
Y	= DFT of a denoised time-frequency representation of an output signal
y	= output signal
ΔT	= sampling time

I. Introduction and Motivation

THE F-18 systems research aircraft (F-18 SRA) is a facility that benefits commercial and military developments at NASA Dryden Flight Research Center. It is now primarily used to develop and test breakthrough technologies, especially in the areas of sensor, actuator, and control system design. The envisioned applications include active flutter suppression, pilot associate systems, advanced displays, massive parallel processing architectures, vehicle management techniques, advanced vehicle system interfaces, and onboard envelope expansion techniques.

The results presented in this paper originate from the latter application. Envelope expansion is a ubiquitous requirement before an aircraft, whether it is military or civilian, may be flown safely and routinely and requires extensive flight tests during which the aircraft gradually operates closer to the boundary of its flight envelope. One of the most catastrophic events that needs to be located during this process is flutter, whereby the aircraft flexible dynamics become unstable through aerodynamic coupling, most often resulting in the loss of the aircraft.[1] Flutter boundary determination is currently done according to the following procedure.

1) A priori finite element structural modeling, combined with simplified expressions for aeroelastic coupling,[1] is used to obtain rough estimates of the flutter boundary as a function of Mach number and dynamic pressure. This analysis is used to draw a conservative flight envelope to be used during flight testing.

2) The flutter boundary estimates and associated flutter mechanisms are then refined during flight tests by closely monitoring the aircraft's flexible dynamics as it evolves toward higher dynamic pressures and Mach numbers. In particular, the damping ratios of the aircraft's flexible modes are closely monitored as indicators of proximity to flutter. Such a practice is standard throughout the industry.[2–4]

The goal of this paper is to address the second step, that is, to provide the flight-test engineer with reliable data to isolate the aircraft's flexible mode shapes and frequencies. Figure 1 shows the excitation and sensor location implemented on the F-18 SRA. Two aerodynamic rotating vanes (named DEI exciters after their manufacturer, Dynamics Engineering, Inc.) are located at both wing tips of the F-18 SRA to excite its flexible dynamics. These aerodynamic vanes can be moved along the wing tips to provide either forward or aft excitation. A picture of the DEI exciter is provided in Fig. 2. During envelope expansion flight tests, these exciters provide oscillatory forces. Typical excitation signals include chirp signals, where the frequency of the exciting force changes gradually with time. The exciters allow the flight-test engineer to explore frequencies ranging from 3 to 40 Hz during flight-test runs that may last up to 60 s. The amplitude of the exciter forces are recorded via strain gauges located close to the exciters. Such technology is widespread in industry and has been used on the DC-10, the L-1011, the Boeing 747, most Airbus aircraft, and many military aircraft, such as the F-16 (Ref. 3). Ten accelerometer sensors are located throughout the body of the aircraft to capture its response. The aircraft is equipped with a sophisticated data acquisition system capable of recording

Received April 18, 1997; revision received Sept. 17, 1997; accepted for publication Sept. 18, 1997.

*Assistant Professor, 33-217, Department of Aeronautics and Astronautics, 77 Massachusetts Avenue. E-mail: feron@mit.edu. Member AIAA.

†Research Engineer, MS 4840D/RS. E-mail: gonzo@xrd.dfrc.nasa.gov. Member AIAA.

‡Associate Professor, 33-103, Department of Aeronautics and Astronautics, 77 Massachusetts Avenue. E-mail: jdpaduan@mit.edu. Member AIAA.

§Research Assistant, 35-223, Department of Aeronautics and Astronautics, 77 Massachusetts Avenue. E-mail: arkasha@mit.edu.

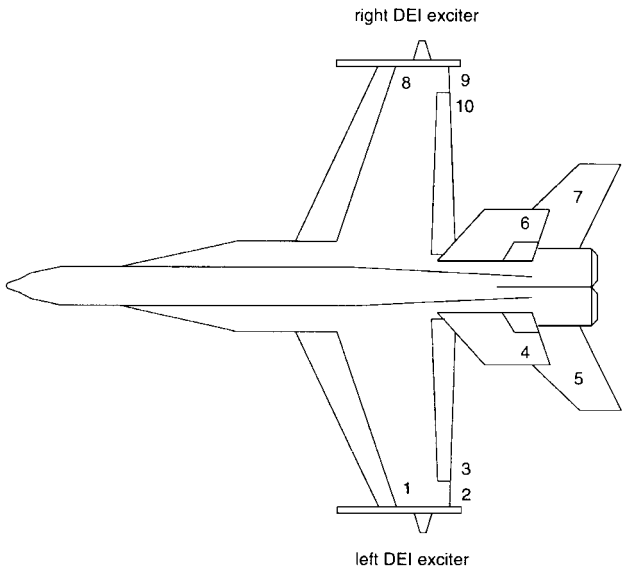

Fig. 1 F-18 SRA exciter and sensor configuration.

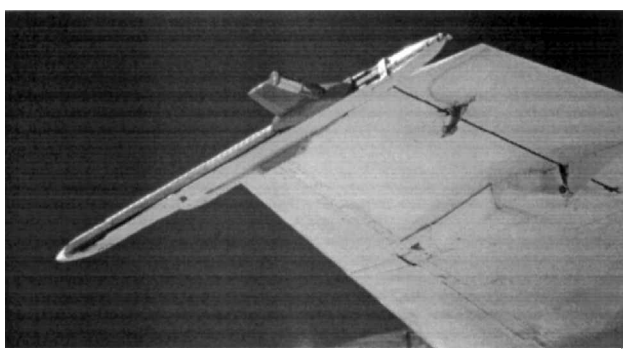

Fig. 2 DEI exciter mounted on F-18 SRA left wing.

and telemetering these data in real time. This exciter/sensor combination allows the flight-test engineer to monitor the linear, flexible dynamics of the aircraft in near real time. Because of the high cost of flying aircraft, it is desirable to make the envelope expansion process as quick as possible. However, this requirement needs to be traded against the accuracy of the identified dynamics, because it is well known that, for time-invariant systems, longer experiments yield better dynamics estimates. When performing flight tests, it is therefore very important for the engineer to use the available data optimally.

From a dynamical systems perspective, determining the flexible dynamics of the F-18 SRA may be seen as a linear system identification problem. Input signals and outputs are measured and available for identification purposes. Both are presumably corrupted by noise arising from unidentified sources that may include engine vibrations, turbulence, or unexpected pilot inputs. Such noise may arise both as process or sensor noise. At steady-state operating conditions, the F-18 SRA is modeled as a linear, time-invariant system.

For such a system, several identification procedures are available. References 5 and 6 contain extensive descriptions of such identification techniques. In particular, spectral estimation techniques with or without time and frequency windowing are very robust identification procedures. If enough data are produced, Welsh's averaged periodograms eventually converge to good transfer function estimates.[7,8]

Other popular identification techniques include the prediction error method (PEM),[5,9] which appears to be very robust as well. Recent and useful additions to these include so-called subspace identification techniques using time-domain input-output data. A detailed description of these techniques may be found in Refs. 10–14 and the references therein. Subspace identification techniques have recently been extended to handle frequency-domain data as well.[15]

With the exception of Fourier analysis, all the methods just mentioned are black-box identification techniques, whose convergence properties have been demonstrated for specific noise categories. In the case of the F-18 SRA, the data are very noisy, and their noise characteristics are neither well known nor necessarily stationary. As a result, it is difficult to trust them. Fourier analysis may be used to cross-check the results of such methods but also tends to be sensitive to the high levels of noise encountered during flight tests. In this paper, it is shown that the particular structure of the exciting chirp signals allows the engineer to obtain enhanced transfer function estimates by allowing the engineer to selectively determine at what time of the flight-test experiment most aeroelastic information is available for a specific frequency. Time-frequency analysis thus stands as the core technique presented and used in this paper. In a different context, time-frequency analysis has already been used in the past for other identification purposes.[16]

This paper is organized as follows. First, time-frequency analysis and its application to chirp signals are presented. Then, it is shown how time-frequency analysis may be used in principle to perform nonlinear noise elimination and enhanced transfer function estimation. The method is then used on experimental data collected from the F-18 SRA. It is compared with existing identification methods, and its efficiency and complementarity with several existing identification procedures are demonstrated.

II. Time-Frequency Analysis of Signals

A. Fourier Analysis

This paper considers sampled-data systems only; all signals are supposed to last from $t = -\infty$ to $+\infty$, taking nonzero values only in the interval $[0, T]$, which corresponds to the duration of the experiment. Define the sampling time ΔT and let N be the smallest positive integer such that $N\Delta T \geq T$. Given a signal $u(t)$, $-\infty \leq t \leq \infty$, the sampled signal will be noted $u_n = u(n\Delta T)$, where n is any unsigned integer. Except for the sampled signal itself, the most common representation of u is its discrete Fourier transform (DFT)[7]

$$\hat{u}(j\omega) = \sum_{n=-\infty}^{\infty} u_n e^{-j\omega n\Delta T}, \qquad \omega \in \boldsymbol{R}$$

$$= \sum_{n=0}^{N} u_i e^{-j\omega n\Delta T}$$

The DFT is very useful because it allows the engineer to observe the frequency content of the signal u. Figure 3 shows the time representations and power spectral densities of typical input and output signals for the F-18 SRA during a flight test performed at 40,000 ft and Mach 0.8. The reader can see that a considerable quantity of information is available from both signal representations; in particular, the power spectral density of the output shows resonances close to 6 and 10 Hz, although not necessarily easy to determine in the latter case because of the presence of high levels of noise. Specific techniques such as signal windowing contribute to smoother transfer functions. However, they also tend to decrease frequency resolution and to distort frequency estimates.

B. Time-Frequency Analysis of Signals

Although the frequency representation $\hat{u}$ is very useful and computationally easy to handle, it does not easily represent signals whose spectral characteristics evolve with time. This is typically the case of chirp signals like

$$u(t) = A\cos[(\dot{\omega}_0 t + \omega_0)t + \phi]$$

This may lead to many lost opportunities if the signal is polluted by broadband noise. This is the reason for introducing time-frequency representations of signals: given a passband filter template b with discrete-time transfer $\hat{b}$, we define the family of passband filters b_{ω_0} defined by

$$\hat{b}_{\omega_0}(\omega) = \hat{b}(\omega - \omega_0)$$

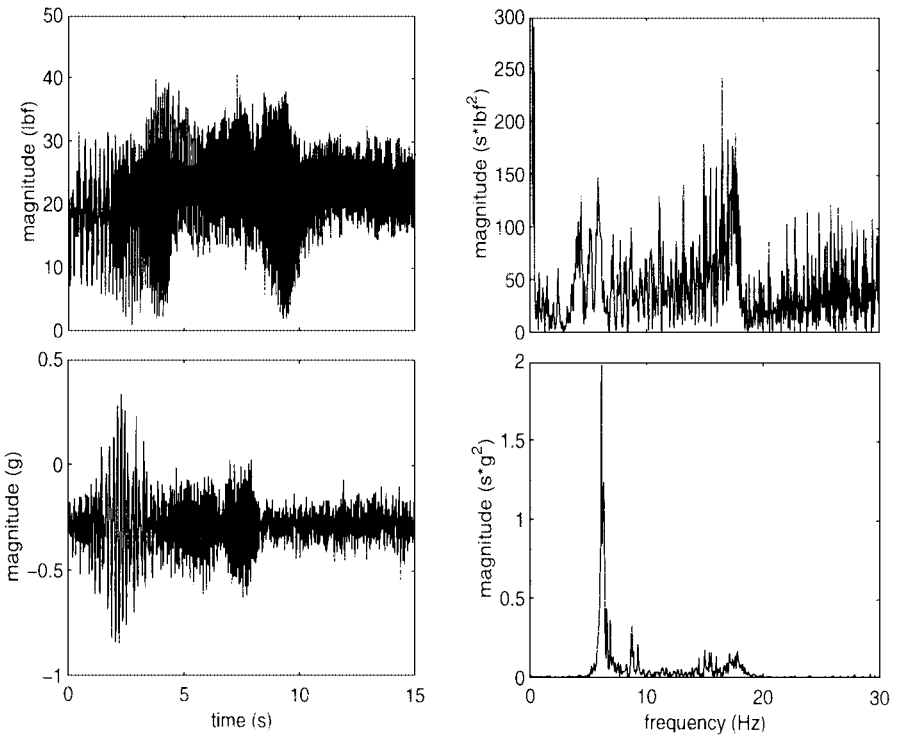

Fig. 3 Time and frequency contents of F-18 SRA: inputs (top) and outputs (bottom).

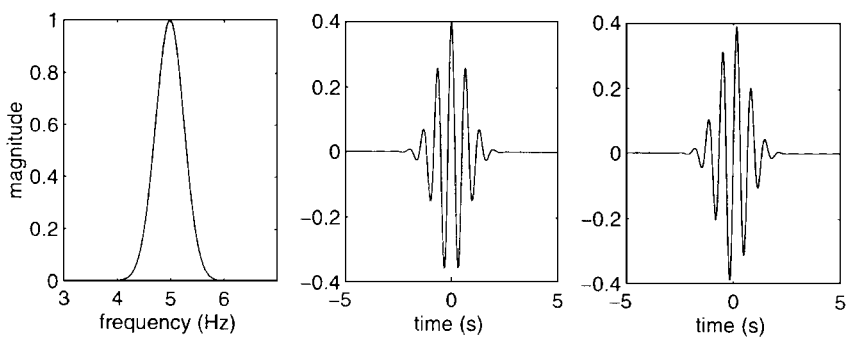

Fig. 4 Morlet wavelet: Fourier transform and impulse response, real (middle) and imaginary (right).

The time-frequency representation $\mathcal{TF}$ of any signal u is then defined by

$$\mathcal{TF}(u, \omega_0, p) = \sum_{n=-\infty}^{n=\infty} u_n b_{\omega_0, p-n} = \left(b_{\omega_0} \star u\right)(p) \tag{1}$$

The transformation $\mathcal{TF}$ therefore maps one-dimensional signals to two-dimensional pictures indexed by time ($p\Delta T$) and frequency (ω_0). When convenient, the shorthands $\mathcal{TF}(u, \omega_0)$ or $\mathcal{TF}(u)$ will be used. This transformation is not unlike wavelet transforms.[17,18] However, the transformation $\mathcal{TF}$ introduced in this paper is not necessarily invertible, although it is linear. Equivalently, the transformation $\mathcal{TF}$ may be seen as filtering the initial signal through a filter bank parameterized by ω_0. Given the sinusoidal nature of the signals involved in the F-18 SRA flight experiments, the Morlet wavelet[19] template was chosen; its transfer function is given by

$$\hat{b}(\omega) = e^{-\lambda\omega^2}$$

In Fig. 4, we have plotted the frequency-domain and (complex) impulse response of b_{ω_0} for $\omega_0 = 10\pi$ and $\lambda = 7$.

By adjusting both parameters, λ and ω_0, it is possible to generate a family of passband filters with arbitrary central frequency ω_0 and bandwidth B, given by $B = \sqrt{[\log 2/(2\lambda)]}$ (measured in radians per second). In traditional wavelet analysis, the scaling factor λ is used primarily to obtain multiresolution information across frequencies such that every decade of the spectrum is covered equally. In the context of this paper, though, λ is kept constant and ω_0 is varied, thus emphasizing a linear scaling of the frequency axis, better suited to structural analyses.

Remark: The reader may wonder about the relationship between the transformation $\mathcal{TF}$ and the short-time Fourier transform (implemented as the Specgram function in the signal processing toolbox of MATLAB[20]). The short-time Fourier transform first truncates the signal in (possibly overlapping) windows and then performs a Fourier analysis of the truncated signals, thus resulting in another time-frequency analysis of the signal. However, the effects of arbitrary signal truncation are well known, including arbitrarily decreased frequency resolution, as well as leveling of resonant peaks. The transformation $\mathcal{TF}$, on the other hand, does not truncate signals a priori.

III. Transfer Function Estimation Using Time-Frequency Analysis

A. Basic Procedure

The time-frequency analysis described earlier suggests the following new transfer function identification procedure whenever chirp-like signals are used for excitation:

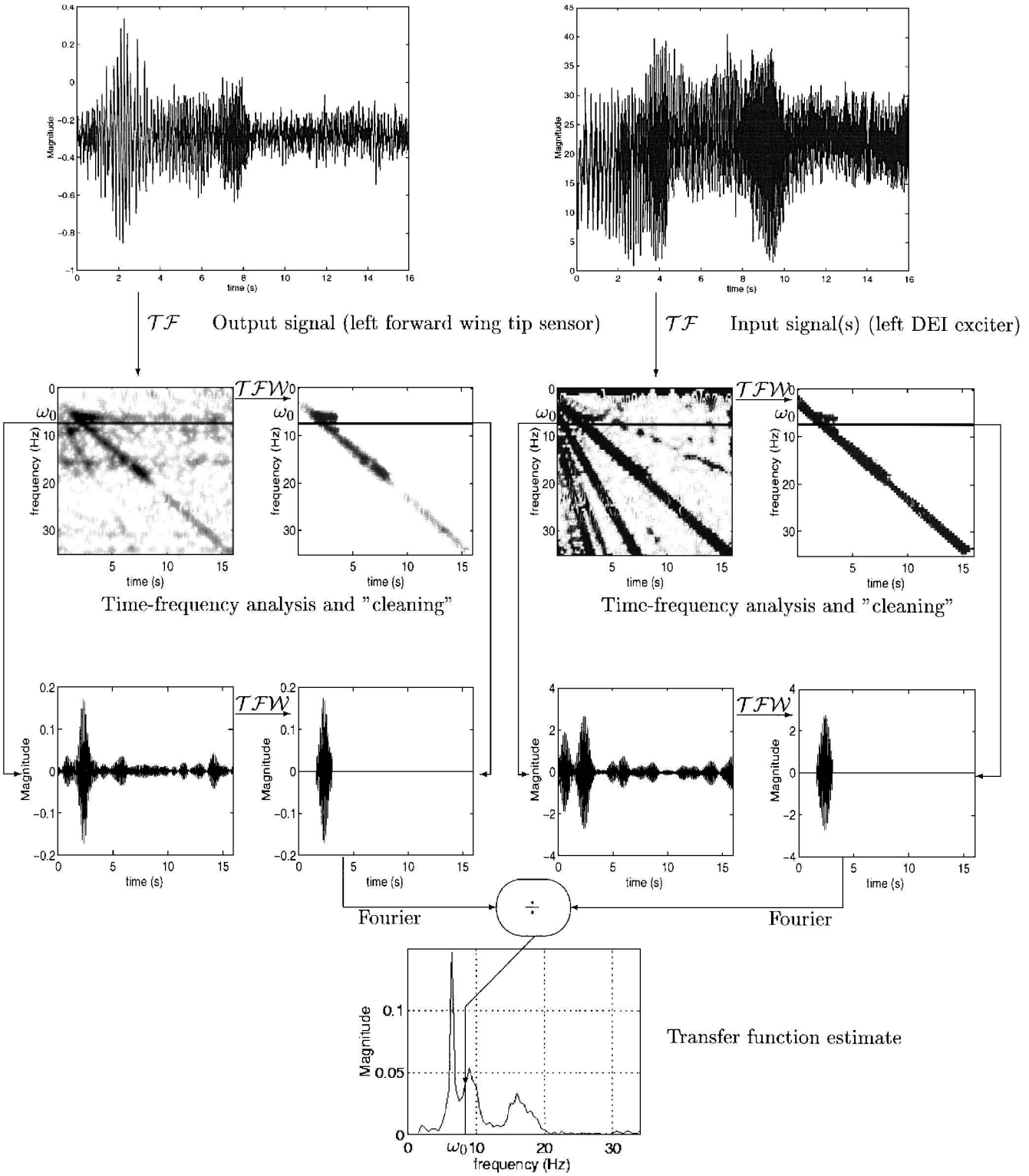

Fig. 5 Transfer function estimation via time-frequency analysis.

1) Perform the time-frequency analysis of both system inputs and outputs.

2) For each frequency of interest, remove the noisy parts of the time-frequency representations.

3) Obtain estimates of the frequency response using the clean time-frequency representations of the signals.

This procedure is illustrated in Fig. 5 and is explained in detail in the following paragraphs.

B. Time-Frequency Analysis and Its Effect on Inputs and Outputs

The F-18 SRA is a multi-input/multi-output system. The flight tests always used the two DEI exciters simultaneously. It is therefore necessary to identify the transfer function from both inputs to a given output simultaneously. In general, we consider the case of a system with m inputs $u_1, \ldots, u_m$ and one output y. Assuming the dynamical system to be linear, there exist linear, single-input/single-output operators $h_1, \ldots, h_m$ such that

$$y = h_1 \star u_1 + \cdots h_m \star u_m \tag{2}$$

The goal of transfer function estimation is to obtain approximations of $h_1, \ldots, h_m$. From Eq. (1), we have

$$\mathcal{TF}(y, \omega) = b_\omega \star y$$

and

$$\mathcal{TF}(u_i, \omega) = b_\omega \star u_i, \qquad i = 1, \ldots, m$$

Consequently, we have

$$\begin{aligned}\mathcal{TF}(y, \omega) &= \sum_{i=1}^{m} \mathcal{TF}(h_i \star u_i, \omega) \\ &= \sum_{i=1}^{m} b_\omega \star (h_i \star u_i) \\ &= \sum_{i=1}^{m} h_i \star (b_\omega \star u_i) \\ &= \sum_{i=1}^{m} h_i \star \mathcal{TF}(u_i)\end{aligned}$$

Thus, the transformation $\mathcal{TF}$ leaves the input-output relation invariant, and the transfer functions h_i, $i = 1, \ldots, m$, may be identified from the transformed inputs and outputs as well.

Time-frequency analysis was applied to the data shown in Fig. 3 using the parameter value $\lambda = 2$. The resulting time-frequency analyses are shown on top of Fig. 5. Only the real part of the transform was plotted. The level of gray is proportional to the amplitude of the output signal. The time-frequency structure of both inputs and output signals appears very clearly. In particular, the chirp structure of the signals appears along with harmonics both at the input and output. In addition, several unidentified signals may be observed. For example, it seems that persistent process noise excites a resonant frequency close to 6 Hz throughout the flight test. Looking simultaneously at both input and output time-frequency representations strongly suggests that the fundamentals of both signals and perhaps the first harmonics are very much correlated.

1. Noise Removal

This procedure is about deciding the useful part of both input and output signals, based on their time-frequency representation $\mathcal{TF}$. As stated in the Introduction, this step currently remains in the hands of the engineer to investigate the full potential of the procedure. The denoising procedure uses the full time-frequency representation of the signal $\mathcal{TF}(u)$ and amounts to setting to zero any element of $\mathcal{TF}(u)$ that appears to represent more noise than actual information. Thus, the noise removal procedure is a manual, time- and frequency-dependent thresholding technique that takes into account the particular structure of the signal. Denote this operation $\mathcal{TFW}(u)$. For a particular frequency ω_0, $\mathcal{TFW}(u, \omega_0)$ thus represents the original signal, filtered through the bandpass filter b_{ω_0} and then time-windowed. This is illustrated in Fig. 5. It has been found experimentally that identical time-windowing of input and outputs yields the best eventual results.

2. Transfer Function Estimation

From the denoised data, the transfer function estimation procedure is straightforward. Assuming no significant information was lost during the noise removal procedure, Eq. (2) suggests that estimates $\tilde{h}_1, \ldots, \tilde{h}_m$ of the transfer functions $h_1, \ldots, h_m$ may be obtained at the frequency ω_0 by solving the equation

$$\mathcal{TFW}(y, \omega_0) = \sum_{i=1}^{m} \tilde{h}_i \star \mathcal{TFW}(u_i, \omega_0) \tag{3}$$

Denoting Y the discrete Fourier transform of $\mathcal{TFW}(y, \omega_0)$ and U_i the discrete Fourier transform of $\mathcal{TFW}(u_i, \omega_0)$, $i = 1, \ldots, m$, we can write Eq. (3) in the frequency domain at the frequency ω_0 as

$$Y(\omega_0) = \sum_{i=1}^{m} \hat{\tilde{h}}_i(j\omega_0) U_i(\omega_0) \tag{4}$$

To obtain these estimates, n independent experiments need to be performed, with $n \geq m$. Let Y^j and U_i^j, $i = 1, \ldots, m$, be the frequency-domain outputs and inputs for the jth experiment. Using Eq. (4), the estimates $\hat{\tilde{h}}_1(j\omega), \ldots, \hat{\tilde{h}}_m(j\omega)$ at frequency ω_0 satisfy the possibly overdetermined linear system

$$Ax = b$$

where

$$A = \begin{bmatrix} U_1^1(\omega_0) & \cdots & U_m^1(\omega_0) \\ \vdots & \ddots & \vdots \\ U_1^n(\omega_0) & \cdots & U_m^n(\omega_0) \end{bmatrix}$$

$$x = \begin{bmatrix} \hat{\tilde{h}}_1(j\omega_0) \\ \vdots \\ \hat{\tilde{h}}_m(j\omega_0) \end{bmatrix}, \qquad b = \begin{bmatrix} Y^1(\omega_0) \\ \vdots \\ Y^n(\omega_0) \end{bmatrix}$$

Estimates may thus be obtained by solving this system in a least-squares sense:

$$x = A^\dagger b$$

where $A^\dagger$ is the pseudoinverse of A.[21]

IV. Application to F-18 SRA Structural Dynamics Identification

The proposed time-frequency analysis is now illustrated using experimental data from the F-18 SRA. For all practical purposes, the F-18 SRA may be considered as a two-input, four-output system, where the only informative outputs are the forward and aft wing tip accelerometers. In this section, we are interested in determining the transfer functions from left and right exciters to the forward left wing tip accelerometer over the frequency range spanning from 5 to 12 Hz.

A. Transfer Function Identification and Comparison with Existing Methods

Six independent experimental measurements are available for the F-18 SRA flying at 40,000 ft and Mach 0.8. These data consisted of ascending and descending frequency sweeps. Each set of experimental data consisted of a symmetric and an antisymmetric run (whereby wing tip actuators were excited either in phase or out of phase). These experimental data were used separately, and the obtained results were crosschecked. The goal of this paragraph is to

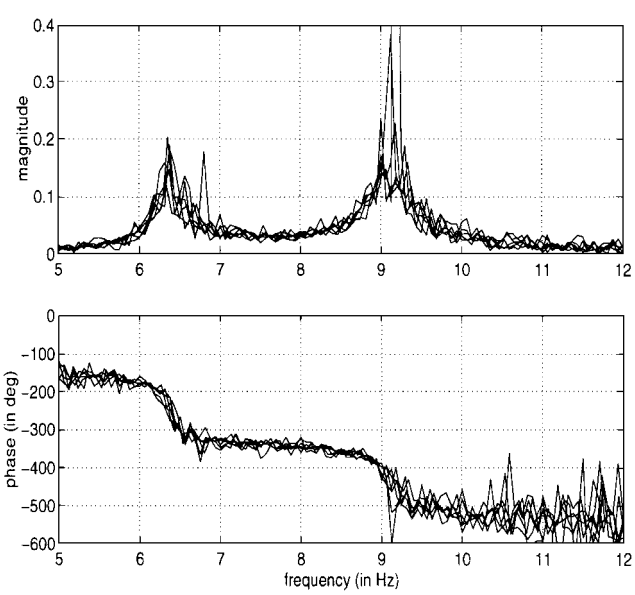

Fig. 6 Transfer function estimates: right exciter to forward left wing tip sensor.

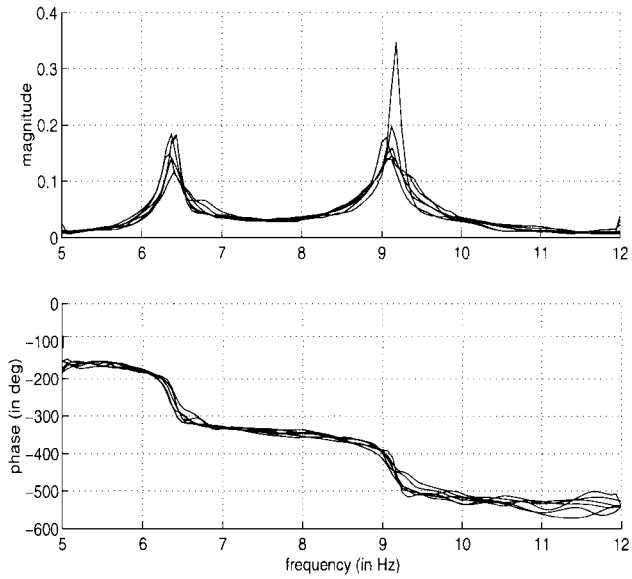

Proposed method

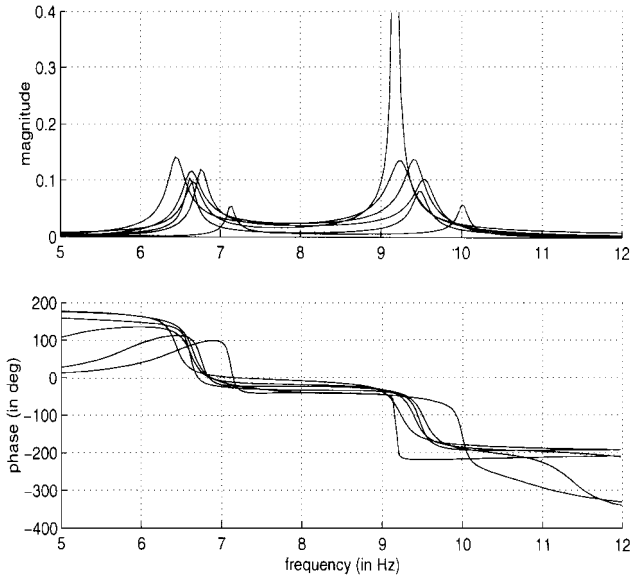

Fourier analysis with frequency-domain subspace ID

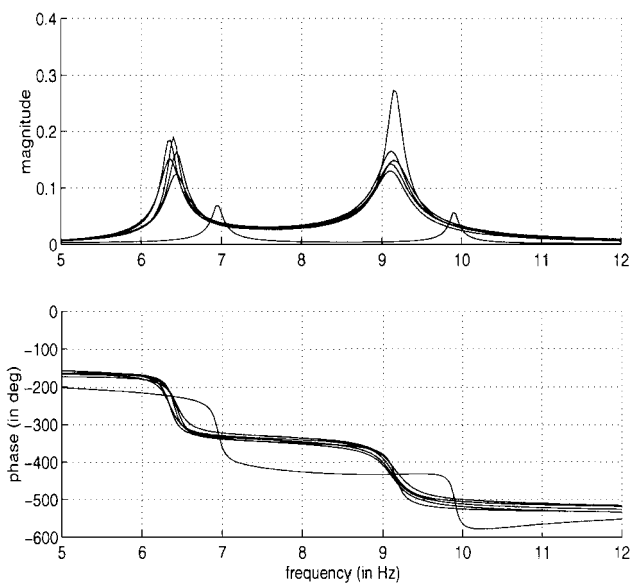

Proposed method and frequency-domain subspace ID

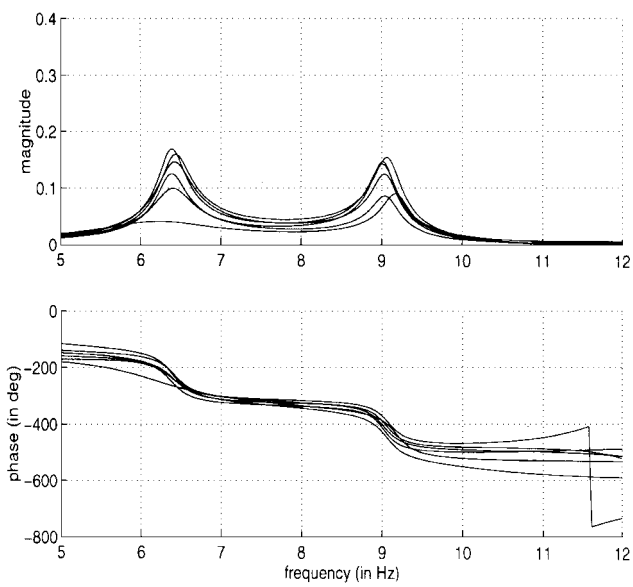

Time-domain subspace ID (N4SID)

Fig. 7 Transfer function estimates: right exciter to forward left wing tip sensor; left vane → left wing forward.

compare the relative performance of the estimation procedure based on time-frequency analysis with other methods. The data were detrended before any further processing. The methods were applied to both unfiltered and filtered (in the 5–12 Hz range) data, and only the best of the two respective results were recorded.

However, note that such comparisons are only indicative of the value of the proposed method. The benchmark identification methods have been chosen from three distinct groups.

1) Direct estimation methods: These comprise the direct transfer function evaluation by using Welch's averaged periodogram method[7,22] and are implemented in the MATLAB signal processing toolbox[20] (spectrum command). The proposed time-frequency analysis described in this paper naturally falls in this category because it may indeed be seen as a smart windowing technique. For the purpose of benchmarking, only full-size windows (corresponding to classical Fourier analysis) were used. Smaller-sized windows[22] yielded no coherent results and were therefore discarded.

2) Parametric estimation methods: These methods are described in detail in Ref. 5 and comprise very well-known methods such as ARMA[23] or PEM.[9] However, these methods did not easily handle multiple data sets (corresponding to separate symmetric and antisymmetric runs). They were therefore discarded for this specific application.

3) Subspace identification methods: These methods are applicable both in the time domain[13] and in the frequency domain.[15] In this paper, the N4SID algorithm presented by Van Overschee and De Moor[13] is used. The frequency-domain algorithm presented by McKelvey et al.[15] is also used: It takes as an input the estimated transfer functions obtained either with simple Fourier analysis or with the proposed time-frequency-based approach. The latter combination is meant to illustrate how the proposed method may be combined with existing identification procedures. For the frequency-domain subspace identification procedure, and following the notation in McKelvey et al.,[15] the parameters were set as follows: system order equal to 4 and number of block rows i equal to 10. This subspace identification algorithm uses transfer function samples as input and produces a state-space model. The chosen transfer functions were from the time-frequency-based estimation procedure and the classical Fourier analysis, respectively.

For the multivariable, time-domain subspace identification procedure N4SID (available on MATLAB[24]), the F-18 SRA experimental data spanned a larger frequency range than necessary. As

a consequence, the presence of resonant modes outside this range resulted in an increased number of states. The best system order was determined to be 14. In addition, and following standard notation,[13] the number of block rows i was chosen to be 20. N4SID had to be modified to account for the presence of multiple data sets (symmetric and antisymmetric runs).[25]

The time-frequency estimation procedure relied on experimental data provided by NASA Dryden exclusively. No a priori model of the aircraft's flexible dynamics was used. Each of the six data sets was denoised following the procedures explained earlier. Denote by $\tilde{h}_{l,i}$ and $\tilde{h}_{r,i}$, $i = 1, \ldots, 6$, the estimated transfer functions from left and right inputs to left forward sensor, respectively. For each of the transfer function estimation methods, the six transfer function estimates $\tilde{h}_{r,i}$, $i = 1, \ldots, 6$, were obtained and are plotted in Figs. 6 and 7. Similar plots were obtained for $\tilde{h}_{l,i}$, $i = 1, \ldots, 6$, but are not presented for lack of space. The quality of transfer function estimates may be evaluated visually and reveals no important difference between the results obtained using the time-frequency analysis, time-frequency analysis completed with subspace identification as presented in McKelvey et al.,[15] and N4SID. One may notice, however, that transfer function phases are more repeatable for the time-frequency-based approaches. These three estimates clearly outperform straight Fourier analysis and Fourier analysis combined with frequency-domain subspace identification.

A quantitative measure of identification performance was performed as follows. Following recommended practices,[5] the transfer function evaluated for each data set was tested against the other five data sets. Specifically, for each of the six data sets, the Fourier transform of the left and right DEI exciter inputs $u_{l,i}$ and $u_{r,i}$ and the forward left wing tip accelerometer output y_i, $i = 1, \ldots, 6$, were computed over the frequency range from 5 to 12 Hz.

The ability of given transfer matrix $[\tilde{h}_{l,i}\ \tilde{h}_{r,i}]$ to repeat a specific data set $u_{l,j}$, $u_{r,j}$, y_j is quantified by the cost function

$$J_{ij} = \sqrt{\int_{\omega=10\pi}^{24\pi} \left| \hat{y}_j(\omega) - \left[\hat{\tilde{h}}_{l,i}(\omega)\ \hat{\tilde{h}}_{r,i}(\omega)\right][\hat{u}_{l,j}(\omega)\ \hat{u}_{r,j}(\omega)]^T \right|^2 \mathrm{d}\omega}$$

For each optimization method, the average performance index

$$J = \frac{1}{30} \sum_{i=1}^{6} \sum_{j=1, j\neq i}^{6} J_{ij}$$

was computed and reported in Table 1.

It may be seen that the proposed approach performs best by this measure of performance. Note, however, that such comparisons are necessarily subjective. A more constructive message is that time-frequency analysis can be included with and benefit any of the aforementioned methods, as has been shown for the case of frequency-domain subspace identification.

B. Operational Use of Time-Frequency Analysis for Flight Testing

In a flight-test environment, time-frequency analysis may be used for a variety of applications.[26] A MATLAB[24]-based application-specific tool named Wavetool[¶] is under development at the Massachusetts Institute of Technology and is targeted at real-time data processing. Wavetool may be used in a number of ways. First, simple time-frequency analysis may be used for standard on-line monitoring of the flutter clearance hardware. Indeed, experience has shown that the DEI exciters may fail, and closely monitoring them can contribute to modify or to abort a mission early if a failure is identified. For example, Fig. 8 shows specific time-frequency analyses of left and right DEI exciters during flight 0554 (following NASA Dryden's archival conventions), performed at Mach 0.9 and 30,000 ft. Figure 8 clearly indicates a failure of the left DEI exciter, because no identified chirp signal may be seen. This failure does not readily show on the time-domain signals alone, also shown in Fig. 8. No exciter failure appears to have been reported during the flight test itself.

[¶]At publication, Wavetool was available at http://web.mit.edu/afs/athena.mit.edu/org/a/aeroastro/www/labs/ICE/projects/wave_tool.html (Oct. 1997).

Transfer function estimation using time-frequency analysis can also be used to confirm some of the natural symmetries of the aircraft dynamics. Referring to Fig. 1, the right exciter should excite the left wing leading-edge sensor the same way the left exciter should excite the right wing leading-edge sensor. Figure 9 was obtained using Wavetool and shows that symmetry is indeed present. Such plots provide extremely valuable information and contribute to build higher levels of confidence in the obtained transfer functions. Note that the presented technique is not limited to linear chirp signals. For example, other experimental F-18 SRA data were collected using so-called logarithmic frequency sweeps instead. Typical time-frequency representations of these may be seen in Fig. 10. Using the appropriate polygons, these time-frequency analyses may be used as well to perform better transfer function evaluations.

Table 1 Performances of different identification techniques on F-18 SRA experimental data

Identification procedure	Cost, g
Proposed approach	1.9039
Fourier analysis	2.9799
Proposed approach and freq. subspace ID	1.9815
Fourier and freq. subspace ID	2.9355
Time-domain subspace ID	1.9927

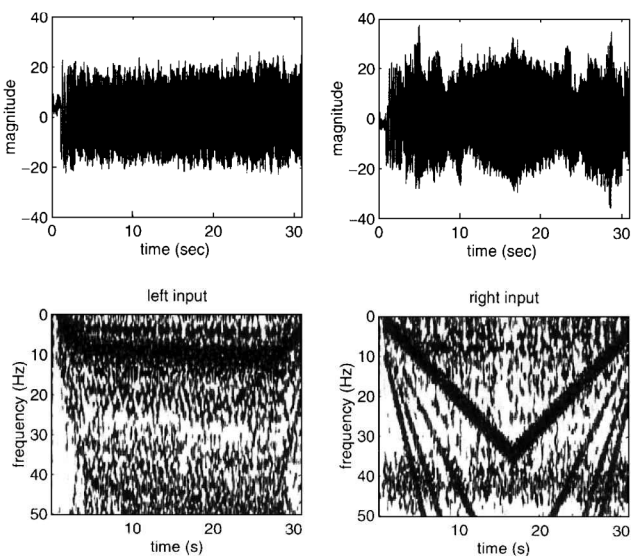

Fig. 8 Left and right DEI exciters, time signals, and time-frequency representations.

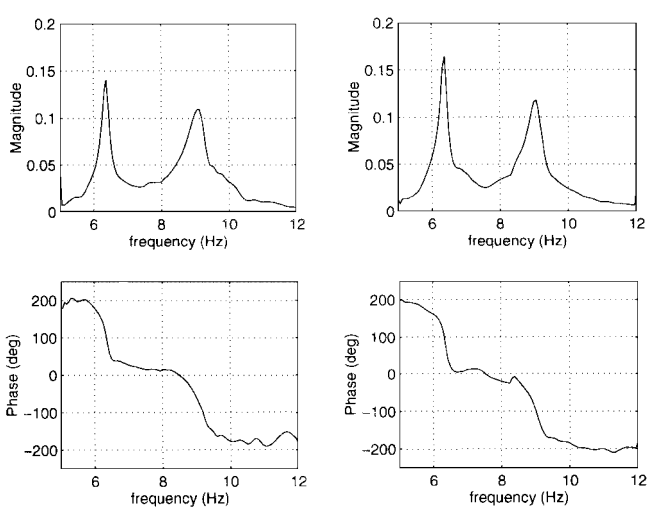

Right exciter to left forward sensor **Left exciter to right forward sensor**

Fig. 9 Transfer functions for symmetric actuator/sensor pairs.

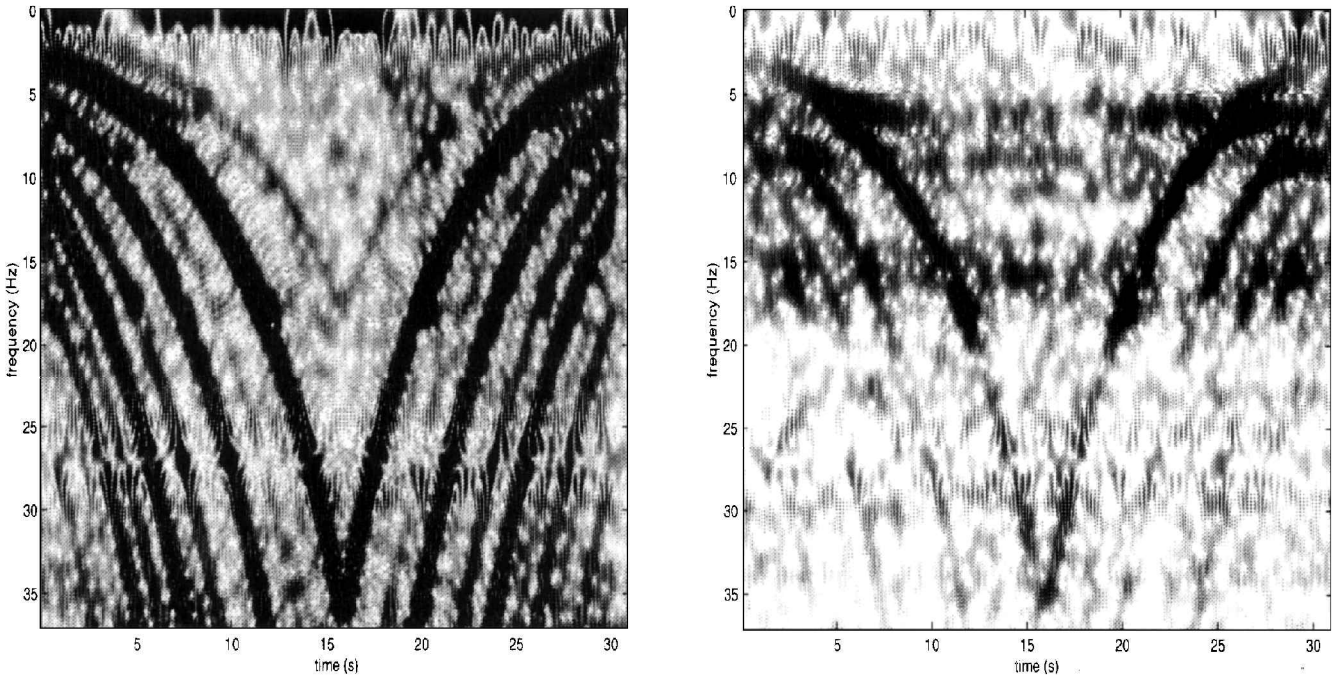

Fig. 10 Logarithmic chirps; flight 0549, Mach = 0.8, and 40,000 ft.

V. Conclusion

Motivated by the flutter clearance problem of NASA Dryden Flight Research Center's F-18 system research aircraft, we presented time-frequency analysis as an efficient tool to identify dynamical systems in the presence of high levels of noise when chirp-like inputs are used by allowing nonlinear noise removal before transfer function estimation. The efficiency and consistency of time-frequency analysis were demonstrated on a numerical example as well as on experimental data arising from the F-18 system research aircraft's flight tests. This article showed that time-frequency analysis can successfully complement other existing identification methods in solving the flutter boundary prediction problem. The proposed transfer function estimation procedure is being implemented in a dedicated application tool and will be tested for routine operation at NASA Dryden Flight Research Center.

Acknowledgments

This research was funded by NASA Dryden Flight Research Center. The authors would like to acknowledge the early contributions of Laurent Duchesne and Xavier Paternot to this research.

References

[1]Bryson, A. E., *Control of Spacecraft and Aircraft*, Princeton Univ. Press, Princeton, NJ, 1994, Chap. 15.

[2]Bucharles, A., Cassan, H., and Roubertier, J., "Advanced Parameter Identification Techniques for Near Real Time Flight Flutter Test Analysis," AIAA Paper 90-1275, May 1990.

[3]Kehoe, M. W., "A Historical Overview of Flight Flutter Testing," NASA TR 4720, Oct. 1995.

[4]Cooper, J., "Parameter Estimation Methods for Flight Flutter Testing," *Proceedings of the 80th AGARD Structures and Materials Panel*, CP-566, AGARD, Rotterdam, The Netherlands, 1995.

[5]Ljung, L., *Subspace Identification: Theory for the User*, Prentice–Hall, Englewood Cliffs, NJ, 1987, Chap. 3.

[6]Pintelon, R., Guillaume, P., Rolain, Y., Schoukens, J., and Van Hamme, H., "Parametric Identification of Transfer Functions in the Frequency Domain: A Survey," *IEEE Transactions on Automatic Control*, Vol. 39, No. 11, 1994, pp. 2245–2259.

[7]Oppenheim, A., and Schafer, R., *Discrete Time Signal Processing*, Prentice–Hall, Englewood Cliffs, NJ, 1989, Chap. 8.

[8]Van der Auweraer, H., Vanherk, P., Sas, P., and Snoeys, R., "Accurate Modal Analysis Measurements with Programmed Sine Wave Excitation," *Mechanical Systems and Signal Processing*, Vol. 1, No. 3, 1987, pp. 301–313.

[9]Ljung, L., "System Identification Toolbox for Use with Matlab: User's Guide," MathWorks, Natick, MA, 1991.

[10]Kung, S., "A New Identification and Model Reduction Algorithm via Singular Value Decompositions," *12th Asilomar Conference on Circuits, Systems and Computers*, Inst. of Electrical and Electronics Engineers, New York, 1978, pp. 705–714.

[11]De Moor, B., Vandewalle, J., Moonen, M., Vandenberghe, L., and Mieghem, P. V., "A Geometrical Strategy for the Identification of State Space Models of Linear Multivariable Systems with Singular Value Decomposition," *Symposium on Identification and System Parameter Estimation*, Pergamon, Oxford, England, UK, 1988, pp. 700–704.

[12]Larimore, W., "Canonical Variate Analysis in Identification Filtering and Adaptative Control," *Proceedings of the 29th Conference on Decision and Control*, Inst. of Electrical and Electronics Engineers, New York, 1990, pp. 596–604.

[13]Van Overschee, P., and De Moor, B., "Subspace Algorithms for the Stochastic Identification Problem," *Automatica*, Vol. 29, No. 3, 1993, pp. 649–660.

[14]De Moor, B., and Van Overschee, P., "N4SID: Subspace Algorithm for Identification of Combined Deterministic Stochastic Systems," *Automatica*, Vol. 39, No. 1, 1994, pp. 75–93.

[15]McKelvey, T., Akçay, H., and Ljung, L., "Subspace-Based Multivariable System Identification from Frequency Response Data," *IEEE Transactions on Automatic Control*, Vol. 41, No. 7, 1996, pp. 960–978.

[16]Tsatsanis, M., and Giannakis, G., "Time-Varying Identification and Model Validation Using Wavelets," *IEEE Transactions on Signal Processing*, Vol. 41, No. 12, 1993, pp. 3512–3523.

[17]Herley, C., Kovacevic, J., Ramchandran, K., and Veterli, M., "Tilings of the Time-Frequency Plane: Construction of Arbitrary Orthogonal Bases and Fast Tiling Algorithms," *IEEE Transactions on Signal Processing*, Vol. 41, No. 12, 1993, pp. 3341–3359.

[18]Strang, G., and Nguyen, T., *Wavelets and Filter Banks*, Wellesley–Cambridge Press, Wellesley, MA, 1996, p. 432.

[19]Daubechies, I., *Ten Lectures on Wavelets*, Society for Industrial and Applied Mathematics, Philadelphia, PA, 1992, p. 76.

[20]*Signal Processing Toolbox User's Guide*, MathWorks, Natick, MA, 1996, p. 6.271.

[21]Golub, G., and Van Loan, C., *Matrix Computations*, 2nd ed., Johns Hopkins Univ. Press, Baltimore, MD, 1989, p. 243.

[22]Pototzky, A. S., Wieseman, C., Hoadley, S. T., and Mukhopadhyay, V., "On-Line Performance Evaluation of Multiloop Digital Control Systems," *Journal of Guidance, Control, and Dynamics*, Vol. 15, No. 4, 1992, pp. 878–885.

[23]Alengrin, G., Bucy, R., Moura, J., Pages, J., and Ribeiro, M., "ARMA Identification," Lab. for Information and Decision Systems, LIDS-P-1588, Massachusetts Inst. of Technology, Cambridge, MA, Aug. 1986.

[24]*Using Matlab*, MathWorks, Natick, MA, 1996.

[25]Duchesne, L., Feron, E., Paduano, J. D., and Brenner, M., "Subspace Identification with Multiple Data Sets," AIAA Paper 96-3716, May 1996.

[26]Brenner, M., and Feron, E., "Wavelet Analyses of F/A-18 Aeroelastic and Aeroservoelastic Flight Test Data," AIAA Paper 97-1216, April 1997.